ACS APPLIED MATERIALS & INTERFACES

RESEARCH ARTICLE

www.acsami.org

High-Resolution X-ray Photoelectron Spectroscopy of Mixed Silane Monolayers for DNA Attachment

Rebecca A. Shircliff,[†] Ina T. Martin,[‡] Joel W. Pankow,[‡] John Fennell,[†] Paul Stradins,[‡] Maria L. Ghirardi,[‡] Scott W. Cowley,[†] and Howard M. Branz*[,‡]

[†]Chemistry and Geochemistry Department, Colorado School of Mines, Golden, Colorado 80401, United States

[‡]National Renewable Energy Laboratory, Golden, Colorado 80401, United States

Supporting Information

ABSTRACT: The amine density of 3-aminopropyldimethylethoxysilane (APDMES) films on silica is controlled to determine its effect on DNA probe density and subsequent DNA hybridization. The amine density is tailored by controlling the surface reaction time of (1) APDMES, or (2) n-propyldimethylchlorosilane (PDMCS, which is not amine terminated) and then reacting it with APDMES to form a mixed monolayer. High-resolution X-ray photoelectron spectroscopy (XPS) is used to quantify silane surface coverage of both pure and mixed monolayers on silica; the XPS data demonstrate control of amine density in both pure APDMES and PDMCS/APDMES mixed monolayers. A linear correlation between the atomic concentration of N atoms from the amine and Si atoms from the APDMES in pure APDMES films allows us to calculate the PDMCS/APDMES ratio in the mixed monolayers. Fluorescence from attached DNA probes and from hybridized DNA decreases as the percentage of APDMES in the mixed monolayer is decreased by dilution with PDMCS.

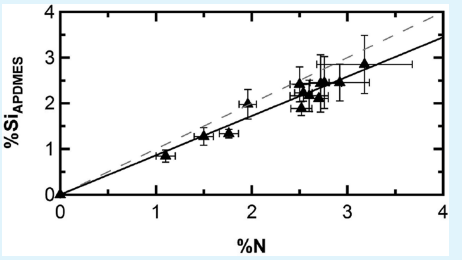

KEYWORDS: XPS, Si 2p, silanes, mixed monolayer, DNA immobilization, DNA hybridization

INTRODUCTION

Chemical modification of silica surfaces with silanes is commonly used for the assembly of thin film devices for applications ranging from DNA microarrays to robotic microhandling.[1−9] These applications employ silane films with functional groups that can selectively bind additional molecules as required.[10] Aminosilanes are of particular interest for DNA microarrays, especially for the covalent attachment of DNA to silica surfaces.[5,8] The surface amine density of aminosilane films in pure or mixed monolayers[11,12] can be tuned through reaction conditions, such as time and concentration,[13] or by dilution with an inert component.[14]

Mixed monolayers can be generated by various deposition techniques that include stepwise deposition[12,14] and codeposition.[15,16] The stepwise deposition technique allows for the direct deposition of a mixed monolayer composed of two silanes that would otherwise react with each other in solution. A submonolayer film of the inert silane is deposited first and then the partially modified surface is reacted with another silane possessing the desired functional group.[14] Determining the composition of mixed monolayers is challenging on silica surfaces.

XPS has been used extensively for elemental and structural analyses of silanized silica surfaces, where the presence of a unique functional group (e.g., an amine) can be used to monitor silane surface coverage.[13] Carbon is a poor indicator of surface coverage because it is a common adventitious contaminant.[17] Nitrogen is intrinsic to aminosilane films and is not an adventitious contaminant, so it is a good indicator of aminosilane deposition.[13] Lee et al. monitor high-resolution XPS N 1s and Si 2p peak intensities to determine the composition of a mixed multilayer film (composed of an aminosilane and a methyl-terminated silane) on an aluminum oxide substrate.[16] It is more challenging to perform this analysis on a silica substrate due to the closeness of the Si substrate and silane peaks.

As an alternative to elemental signatures, changes in chemical-bonding-specific component peaks can also be used to characterize silane coverage. Previously, Pleul et al. demonstrated that silane surface coverage can be characterized via analysis of the high binding energy Si 1s peak (1840 eV) using a special Ag Lα X-ray source.[18] Conventional, commercial spectrometers are limited by the photon energy of an Al Kα source (1486.6 eV).[19] We show that fitting the more commonly measured high-resolution XPS Si 2p peak (~102 eV) can yield a component peak indicative of a silane attached to silica. Our technique is particularly useful for silanes, such as PDMCS, that do not possess distinguishable elemental signatures after surface attachment.

Alexander et al. demonstrate that the Si 2p component peaks in $Si(-O)_x$ films can be resolved and quantitative peak fitting can be performed based on two assumptions: 1) each Si atom has a valence of four, resulting in four component peaks within the Si 2p envelope and 2) the shift of the Si binding energies depends primarily on the number of oxygen atoms attached to the Si.[20] The four component peaks of the Si 2p envelope are referred to

Received: August 17, 2010
Accepted: July 28, 2011
Published: July 28, 2011

as $Si(-O)_1$, $Si(-O)_2$, $Si(-O)_3$, and $Si(-O)_4$, where the oxygen subscript indicates how many oxygen atoms are attached to the Si atom. Alexander et al.'s deconvolution is widely used to curve fit the Si 2p peak envelope and to characterize $Si(-O)_x$ containing films on solid surfaces.[21−25]

Analytical techniques such as XPS are needed to determine how surface composition affects the degree of attachment of subsequent molecules such as DNA. Control of surface functionality has the potential for improving the attachment of DNA.[15,26] Several studies show lower DNA hybridization efficiencies on modified surfaces with high probe (immobilized ssDNA) densities.[27−30] The cause of these lowered efficiencies is uncertain, but various explanations point to probe−probe interactions and electrostatic repulsion between the DNA probe layer and incoming targets,[30] thermodynamic stability of the probe−target complex[31] and intermolecular interactions between DNA strands.[27]

For this study, we generated both pure APDMES and PDMCS/APDMES mixed monolayers with varying APDMES densities. The mixed monolayers are generated in a stepwise deposition by first varying the substrate exposure to PDMCS, which controls the unmodified surface area available for subsequent APDMES attachment. By monitoring the high-resolution XPS N 1s and Si 2p spectra, we are able to measure the mixed monolayer composition. Fluorescence assays are used to monitor both DNA immobilization and DNA hybridization on the mixed monolayers. Our work shows that (1) high-resolution XPS measurements of the $Si(-O)_1$ component within the Si 2p peak can effectively quantify silane coverage on silica, (2) the composition of mixed silane monolayers can be determined using the $Si(-O)_1$ method we developed and (3) the $Si(-O)_1$ method is useful for determining the relationship between surface amine density and subsequent DNA attachment.

EXPERIMENTAL METHODS

Materials. All reagents purchased were used as received, unless otherwise noted. Anhydrous toluene, ACS reagent grade toluene, sodium dodecyl sulfate (SDS), formamide, dithiothreitol (DTT), Alconox and phosphate buffer components were purchased from Sigma-Aldrich. Dichloromethane, 2-propanol and sodium hydroxide pellets were purchased from J.T. Baker. Anhydrous ethanol was purchased from Pharmco-Aaper. n-Propyldimethylchlorosilane and 3-aminopropyldimethylethoxysilane were purchased from Gelest, Inc. N-[e-Maleimidocaproyloxy]sulfosuccinimide ester (Sulfo-EMCS) was purchased from Pierce Biotechnology. Saline sodium citrate (SSC) was purchased from Fisher Scientific. Bovine serum albumin (BSA) was purchased from Research Organics. Silicon wafers with ~270 nm of thermally grown silicon dioxide were purchased from University Wafers.

Preparation of Silane-Modified Substrates. The reaction conditions we use for silane attachment are well-established[13,32] for generating stable, chemically bonded silane films on silica surfaces. All silane treatments were performed on the oxidized silicon wafers after they were cleaned with a 1% (w/v) solution of Alconox in deionized water, cut into ~2 cm^2 samples and then cleaned by oxygen plasma for 5 min at 154 W in a Technics 500-II Plasma System. Spectroscopic ellipsometry measurements of plasma-cleaned oxidized silicon wafers showed that the oxide thickness was 267 nm, as specified by the manufacturer. We confirmed that exposure of the silica substrate to toluene (solvent for silane reaction) for 19 h did not change the silica layer thickness.

Figure 1 shows the molecular structures for APDMES and PDMCS silane molecules, in addition to a schematic of a PDMCS/APDMES mixed monolayer. After cleaning, pure APDMES and pure PDMCS monolayers were formed by exposure to a 1% (v/v) silane solution in anhydrous toluene at 60−65 °C for times varying from 15 s to 19 h. The PDMCS/APDMES mixed monolayers were generated via a stepwise deposition sequence, in which clean, oxidized silicon wafers samples were first exposed to a 1% (v/v) PDMCS solution in anhydrous toluene at 60−65 °C for times ranging from 15 s to 19 h. After postsilanization washes, PDMCS-treated samples were then exposed to a 1% (v/v) APDMES solution in anhydrous toluene at 60−65 °C for 19 h. This procedure is designed to obtain consistent total silane coverage of the surface, while varying only the degree of amine functionality. Postsilanization washes, which are used to wash off any unreacted or dimerized silane, consisted of 5 min washes in toluene, dichloromethane and anhydrous ethanol, followed by an anhydrous ethanol rinse and drying under nitrogen. During silane treatment, each sample was placed in a separate test tube and sealed with a septum. All glassware was cleaned in a base bath (1 M sodium hydroxide dissolved in isopropanol) overnight and dried at 120 °C prior to use.

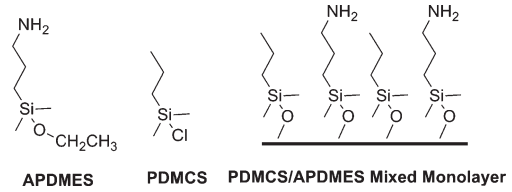

Figure 1. PDMCS and APDMES molecular structures and schematic of a PDMCS/APDMES mixed monolayer.

AFM images show that pure APDMES and PDMCS/APDMES mixed monolayers generate a uniform surface coating on the silica substrate with roughness values below 6 Å in all cases (see Figure S1 in the Supporting Information). Spectroscopic ellipsometry measurements on the saturated pure APDMES and PDMCS/APDMES mixed monolayers indicate a single monolayer is formed for all films with thicknesses of 0.6 ± 0.2 nm and 0.8 ± 0.2 nm, respectively, both of which approach the theoretical monolayer thickness of an APDMES film (0.7 nm).[8] Additionally, PDMCS molecules contain a unique Cl atom that would be easily detected by XPS if unhydrolyzed PDMCS were physisorbed to the surface. Cl was not detected on any of the PDMCS-treated samples ruling out extensive physisorbed PDMCS on the surface (XPS detection limit >0.1%).

Modification of Silanized Substrates with Heterobifunctional Cross-Linker. Silanized substrates were treated with a 1 mM solution (0.41 mg/mL) of Sulfo-EMCS dissolved in sodium phosphate buffer (0.1 M, pH 7.2−7.5) for 40 min at room temperature per vendor recommendations.[33] After cross-linker addition, samples were washed for 10 min each in two separate washes of sodium phosphate buffer (0.1 M, pH 7.2−7.5), rinsed with DI water and dried under nitrogen.

Spectroscopic Ellipsometry and Atomic Force Microscopy. Silane film thicknesses were measured with a spectroscopic ellipsometer (J.A. Woollam alpha-SE). Spectroscopic ellipsometry is used to determine the thickness of silane films by modeling them as "silica-like".[13,34,35] It is assumed that the silane layer refractive index is approximately equal to that of silica (n = 1.465).[13] The silicon dioxide thickness is subtracted from the calculated total thickness of a silane/SiO_2 layer to yield the silane film thickness. Atomic Force Microscopy (AFM) images are acquired in tapping mode on a Scanning Probe Microscope DI 3100 with a Nanoscope V controller from Veeco Metrology, using Si tips. Note: all AFM images are in the Supporting Information.

X-ray Photoelectron Spectroscopy. Silane films were characterized with XPS using a Physical Electronics PE5800 ESCA/AES system. Reported XPS values and error bars are the average and standard

Table 1. Oligonucleotide Sequences and Terminus Modifications

oligo name	sequence (5′- 3′)	length	5′- modification	3′- modification
oligo 1	CCCAGGAATGCCCAGCCAA	19	FAM	thiol
oligo 2	CCCAGGAATGCCCAGCCAA	19	FAM	none
oligo 3	CCCAGGAATGCCCAGCCAA	19	Thiol	none
oligo 4	TTGGCTGGGCATTCCTGGG	19	FAM	none
oligo 5	ACAAACCCATGCCGGCTAA	19	FAM	none

deviation of two to three measurements each on at least two independent samples. For calculated values, errors were propagated using standard statistical analysis. Spectra were collected using a monochromatic Al Kα X-ray source (1486.6 eV, 7 mm filament operated at 350 W), hemispherical analyzer, and multichannel detector. A low-energy (~1 eV) electron flood gun was used for charge neutralization. To correct for residual sample charging, high-resolution spectra were charge referenced by setting the C 1s hydrocarbon peak to 284.8 eV. Survey spectra were collected using an analyzer pass energy and step size of 187.85 eV and 0.8 eV/step, respectively.[36] High-resolution spectra were collected using an analyzer pass energy of 23.50 eV and a step size of 0.1 eV/step. Curve fitting was performed using CasaXPS software (www.casaxps.com) with a GL(30) fit. Component peak positions were based on the results by Alexander et al.,[20] who reported the binding energies of $Si(-O)_1$, $Si(-O)_2$, $Si(-O)_3$, and $Si(-O)_4$ to be 101.5, 102.1, 102.8, and 103.4 eV, respectively. Full widths at half-maximum (FWHM) for the Si 2p component peaks were constrained to be equal and varied from 1.6 to 1.7 eV. The default relative sensitivity factor (RSF) values supplied by the XPS manufacturer were used for determining the atomic concentrations (%AC) of the surface composition. The photoelectron takeoff angle (TOA), which is defined relative to the surface plane, was set to 15° for all spectra. For perspective, analysis of the Si 2p peak in poly(methyl methacrylate) samples with an Al Kα X-ray source at TOAs of 10, 45, and 90° (relative to surface plane) yielded sampling depths of 1.7, 6.9, and 9.7 nm, respectively.[17]

Oligonucleotide Sequences. Synthetic DNA, with the desired modifications at the 5′ and 3′ ends, was purchased from Integrated DNA Technologies (IDT); IDT purified the DNA by high-performance liquid chromatography (HPLC). We selected the oligonucleotide sequences shown in Table 1 for their ability to form stable hybrids with their complementary strand at room temperature. In addition, the selected sequences have low probability of self-forming a secondary structure.[37] Oligo 1 is a 3′-thiol-modified probe that can covalently bond to the cross-linker attached to the silica surface. This covalent attachment was detected via fluorescent labeling with 5′-fluorescein phosphoramidite (5′-FAM). To determine whether the signal from oligo 1 was due to covalently bound DNA or nonspecific adsorption, oligo 2 was used as a negative control. Oligo 2 has the same sequence as oligo 1, but does not have a thiol modification. Therefore, oligo 2 cannot covalently bind to the surface, but any intermolecular interactions (nonspecific adsorption) between the DNA bases and the surface can be detected due to the 5′-FAM modification. In order to maintain the same DNA-labeling protocol (5′-FAM modification) for fluorescence detection of both immobilization and hybridization assays, oligo 3 was used instead of oligo 1 in hybridization studies. Oligo 3 is a 5′-thiol-modified probe, without a FAM label, that will covalently attach to the cross-linked surface. Note that oligos 1 and 3 have the same sequence, but the thiol modification of the probes changes from the 3′ to the 5′ terminus, respectively. The covalent attachment of oligo 3 was determined through the hybridization of the cDNA target, oligo 4. Oligo 4 is the complementary target to oligo 3, and formation of the DNA duplex was detected via 5′-FAM labeling. To confirm that a DNA duplex was formed due to hybridization between oligos 3 and 4, we used oligo 5 (noncomplementary to oligo 3) as a negative control.

DNA Immobilization. Thiol-modified DNA sequences, which were protected with a disulfide bond by the vendor, were reduced to the sulfhydryl active form by incubating the sample with 0.1 M DTT dissolved in sodium phosphate buffer (0.1 M, pH 8.3−8.5) for 1 h at room temperature. After reduction of the sample, the DNA was desalted using Illustra NAP-5 columns (GE Healthcare) according to vendor specifications. For DNA immobilization, probes were resuspended at 20 μM concentration in sodium phosphate buffer (0.1 M, pH 7.2−7.5) and 10 μL drops were pipetted onto modified substrates and allowed to incubate for 2 h at room temperature in a humid Petri dish. Following incubation, substrates were washed for 5 min each in 0.1% SDS + 2× SSC, followed by 0.1% SDS + 1x SSC and finally 0.1% SDS + 0.5× SSC. After the washes, the samples were rinsed with DI water and dried under nitrogen.

DNA Hybridization. After DNA immobilization, the samples were treated with a prehybridization buffer (5x SSC, 25% formamide, 0.1% SDS, 0.1 mg/mL BSA) for 1 h at 42 °C to prevent nonspecific adsorption by blocking all active surface sites (e.g., amine) that could interact with the target. After prehybridization treatment, samples were washed with 0.1x SSC twice for 5 min, then rinsed with DI water and dried under nitrogen. For DNA hybridization, samples were exposed to 10 μL drops of 1 μM target suspended in 4× SSC + 0.1% SDS for 2 h at room temperature. Samples were then washed with 4× SSC + 0.1% SDS for 5 min; followed by two, 5 min washes in 2× SSC + 0.1% SDS, then a 1 min wash each in 0.2× SSC and 0.1× SSC.[37] After the washes, samples were rinsed with DI water and dried under nitrogen.

Fluorescence Imaging. Samples with fluorescently labeled DNA attached to the surface were analyzed using a Typhoon 9400 Variable Mode Imager (GE Healthcare). Reported fluorescence values and error bars are the average and standard deviation, respectively, of three measurements from at least four independent samples. Scanner settings for FAM-labeled samples were set to a 488 nm excitation wavelength with a 520 nm emission filter (40 nm bandpass) and a sensitivity of 500 V for the photomultiplier tube (PMT). Macroscopic spots of fluorescently labeled DNA on samples were imaged with a resolution of 100 μm and the fluorescence was analyzed using ImageQuant software (v. 5.2, GE Healthcare).

RESULTS AND DISCUSSION

$Si(-O)_1$ Component Peak as a Measure of Silane Surface Coverage. The Si 2p binding energy is sensitive to the number of O atoms bonded to Si, therefore the covalent attachment of a silane to SiO_2 can be distinguished from the underlying SiO_2 substrate.[20,21,25] High-resolution XPS Si 2p spectra of silica exposed to APDMES for (A) 15s and (B) 480 min are shown in Figure 2. Curve fitting, based on the conventions of Alexander et al.,[20] shows the presence of two peaks; the larger peak at 103.0 ± 0.1 eV is assigned to the silicon associated with oxygen within the silica substrate, as it is consistent with a $Si(-O)_4$ component peak. The smaller peak at 101.1 ± 0.1 eV is assigned to the $Si(-O)_1$ component peak, which is indicative of APDMES bonded to the silica surface. These spectra show that the area of the $Si(-O)_1$ component increases with increasing substrate exposure time to APDMES.

The atomic concentration of an element is the number or mole percent of that element relative to all elements detected within the XPS information depth, as described in detail elsewhere.[17] For example, the atomic concentration of Si (%Si) represents the percentage of all Si atoms, including those in the silica substrate and in the bonded silane molecules, relative to the total number

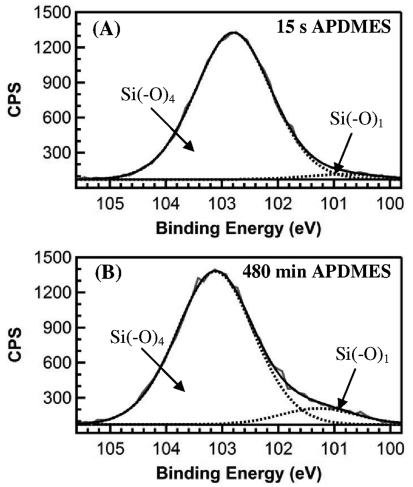

Figure 2. Si 2p high-resolution XPS spectra for pure APDMES films on silica after exposure times of (A) 15 s and (B) 480 min to APDMES. Dotted lines show fits corresponding to the $Si(-O)_4$ component from the silica substrate and the $Si(-O)_1$ component from APDMES attachment.

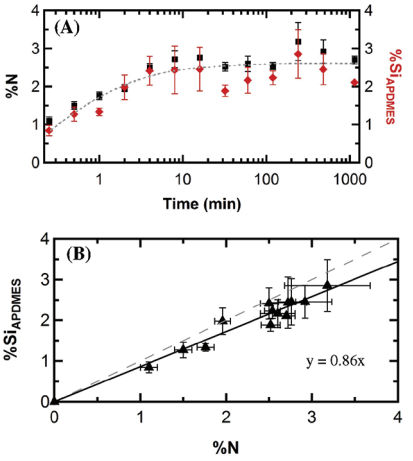

Figure 3. (A) Dependence on exposure time to APDMES of %N (black squares) and $\%Si_{APDMES}$ (red diamonds) in pure APDMES monolayers. Dashed line drawn as a guide for the eye to both data sets. (B) $\%Si_{APDMES}$ and %N in pure APDMES monolayers, with a linear best-fit line (solid black) and 1:1 fit line (dashed gray) for reference. All values are determined by high-resolution XPS.

of Si and non-Si elements. Further, the atomic concentration of the Si atoms in the information depth that are from APDMES molecules ($\%Si_{APDMES}$) can be calculated using:

$$\%Si_{APDMES} = \%Si \frac{A_{Si(-O)_1}}{A_{Si_{2p}}} \quad (1)$$

where %Si is the atomic percent Si, $A_{Si(-O)1}$ is the $Si(-O)_1$ peak area and A_{Si2p} is the total Si 2p peak area ($Si(-O)_1 + Si(-O)_4$).

Figure 3A shows an increase in the $\%Si_{APDMES}$ detected as the sample exposure time to APDMES is increased. Both the $\%Si_{APDMES}$ and the atomic concentration of nitrogen (%N) within the XPS information depth increase at the same rate and nearly triple between 15 s and 480 min exposure times, indicating an increase in the APDMES surface coverage. The APDMES surface coverage appears to reach saturation after less than 100 min of APDMES exposure, even with excess silane in solution.[38]

Figure 3B plots $\%Si_{APDMES}$ versus %N (both from Figure 3A). Negative control samples, which were not exposed to APDMES, showed no presence of nitrogen or the $Si(-O)_1$ peak moiety on the surface. There is a clear linear correlation between these two elements, resulting in the experimental relationship:

$$\%Si_{APDMES} = 0.86 \cdot \%N \quad (2)$$

This is close to the expected 1:1 ratio of Si:N in the APDMES molecule. The small deviation from unity slope could be due to our choice of peak shapes in the peak fitting, the relative signal-to-noise ratio of each element, RSF inaccuracies or attenuation of the Si 2p signal by the APDMES layer. For the pure APDMES system, the slope 0.86 defines the relative sensitivity of XPS to $\%Si_{APDMES}$ and %N; we will use this slope to determine $\%Si_{APDMES}$ even when other silanes without a marker are also present (e.g., PDMCS).

Previously, the Si 2p peak was thought to be an unreliable technique for monitoring accurate surface coverage due to background Si signal[39] or poor resolution of the peak.[40−42] One earlier study[18] demonstrated a direct correlation between the nitrogen signal and the silane contribution to the Si 1s peak. However, the silane contributions to the silicon signal in the Si 2p peak were not resolved. Our curve fitting demonstrates that the $Si(-O)_1$ silane peak is an excellent indicator of silane coverage over a wide range of exposure times.

In addition to examining the relative atomic composition of the APDMES films, we also calculated the surface density ($\Gamma_{monolayer}$) of the saturated monolayer using the method presented by Bramblett et al.[43] Here,

$$\Gamma_{monolayer} = \frac{t\rho a N_{AV}}{MW} \quad (3)$$

where t is the overlayer thickness (0.6 ± 0.2 nm for APDMES, as measured by spectroscopic ellipsometry), ρ is the APDMES density (0.857 g/cm^3; specified by manufacturer Gelest), a is the conversion factor (10^{-21} cm^3/nm^3), N_{AV} is Avogadro's number and MW is the molecular weight of APDMES without the hydrolyzable ethoxy group (116 g/mol). Using this equation yields a monolayer density of 2.7 ± 0.9 APDMES molecules/nm^2. For comparison, we also estimated the surface density of APDMES molecules using XPS data as

$$\Gamma_{monolayer} = \frac{A_{Si(-O)_1}}{A_{Si_{2p}}} n_{SiO_2} z \quad (4)$$

where z is the sampling depth for XPS at a specified takeoff angle (2.1 nm for a 15° takeoff angle),[44] n_{SiO_2} is the molecular concentration of silica (22 SiO_2 molecules/nm^3), and $A_{Si(-O)1}/A_{Si2p}$ is the area fraction of the $Si(-O)_1$ peak to the entire Si 2p peak (0.09 ± 0.01 for a sample exposed to APDMES for 480 min; see Figure 2B). This calculation results in 4.2 ± 0.5 APDMES molecules/nm^2. Note that n_{SiO_2} is based on the density of thermal SiO_2 (2.2×10^{-21} g/nm^3).[45] The actual sample density is lower because it is a combination of SiO_2 and APDMES density. We estimate an ~2:1 ratio of SiO_2:APDMES, which lowers $\Gamma_{monolayer}$ to 3.3 APDMES molecules/nm^2. This 2:1 ratio is based on the 2.1 nm sampling depth of the XPS, the APDMES layer thickness (0.6 nm) and the unit cell thickness of SiO_2 (0.7 nm). It is important to note that this calculation does not include effects of electron attenuation of the underlying SiO_2 by the APDMES layer; electron attenuation lengths are required for

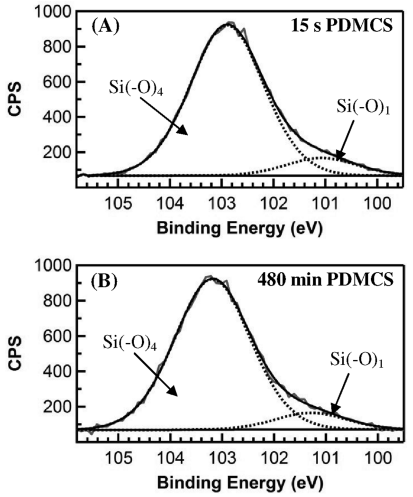

Figure 4. Si 2p high-resolution XPS spectra for PDMCS/APDMES mixed monolayer films on silica after a (A) 15 s and (B) 480 min exposure to PDMCS, followed by a 19 h exposure to APDMES. Dotted fit curves show the $Si(-O)_4$ component from the silica substrate and the $Si(-O)_1$ component from silane molecule attachment.

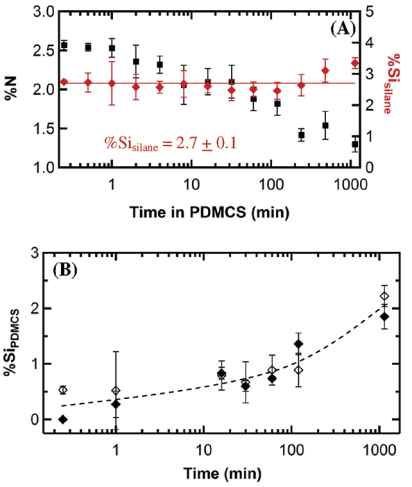

Figure 5. (A) Dependence of %N (black squares) and $\%Si_{silane}$ (red diamonds) on PDMCS exposure time for PDMCS/APDMES mixed monolayer films. (B) Dependence of $\%Si_{PDMCS}$ in pure PDMCS monolayers (closed diamonds) and mixed monolayers (open diamonds) on PDMCS exposure time. $\%Si_{PDMCS}$ in the mixed monolayers was calculated from Figure 5A data and eq 6. Dashed line drawn to guide the eye for both data sets. All values are determined by high-resolution XPS.

an absolute measurement.[46] Lastly, we assume that the RSFs are similar for Si from the SiO_2 and APDMES. Since this instrument has been used to measure accurate Si:O ratios in both thermal silica and soft polymers (polydimethylsiloxane),[47] this is a reasonable assumption. Our calculated values correspond well with the number of OH surface sites available for silane attachment on silica (~5 OH molecules/nm^2)[48] and values from Kallury et al. who reported 2−4 APDMES molecules/nm^2 for APDMES monolayers on silica.[49]

Determination of Mixed-Monolayer Composition using $Si(-O)_1$ Component Peak. Because PDMCS has the same type of covalent bond to the silica surface as APDMES, attachment of either molecule yields the same $Si(-O)_1$ component peak at 101.1 eV in high-resolution XPS spectra. Figure 4A shows the total $Si(-O)_1$ component peak area that represents attachment of both PDMCS and APDMES to the silica surface after a short (15 s) predeposition of PDMCS, followed by a 19 h APDMES exposure. The same size $Si(-O)_1$ component peak is observed in Figure 4B, where the predeposition time of PDMCS is 480 min, but the APDMES exposure time is again 19 h. Thus, the total silane surface coverage is not changing significantly (although the film composition is, as discussed below). Si 2p high-resolution XPS spectra of pure PDMCS monolayers are also identical to those shown in Figure 4A, B (see the Supporting Information, Figure S2). In all three of these cases, the silane coverage of the silica surface is the same.

Figure 5A shows the effect of PDMCS exposure time on %N and $\%Si_{silane}$ for PDMCS/APDMES mixed monolayer films. Similar to eq 1, $\%Si_{silane}$ is calculated using

$$\%Si_{silane} = \%Si\frac{A_{Si(-O)_1}}{A_{Si_{2p}}} \quad (5)$$

where %Si is the atomic percent Si, $A_{Si(-O)_1}$ is the $Si(-O)_1$ peak area and $A_{Si_{2p}}$ is the total Si 2p peak area. Figure 5A demonstrates that the $\%Si_{silane}$ remains nearly constant at 2.7 ± 0.1%, whereas the %N of the mixed monolayer film decreases as the PDMCS predeposition time is increased. The 19 h APDMES exposure ensures a consistent, saturated silane film while the time in PDMCS (before APDMES) provides control of amine density. A slight increase in the $\%Si_{silane}$ is observed for the highest predeposition times; it is possible that the 19 h predeposition of PDMCS yields a slightly higher total silane surface coverage. In addition, Figure 5A shows a %N of ~0.8 in the mixed monolayer even after a 19 h (1140 min) predeposition of PDMCS. Thus, complete monolayer coverage with PDMCS was not reached even after 19 h.

To further examine PDMCS surface coverage, we deposited a series of PDMCS-only films at varying exposure times. The $\%Si_{PDMCS}$ in pure PDMCS monolayers can be determined from the XPS data using eq 5; in these films only PDMCS contributes to the $Si(-O)_1$ peak. These data are shown in Figure 5B (closed diamonds). The $\%Si_{PDMCS}$ in the pure PDMCS monolayers increases with increasing exposure time; the lack of saturation supports that PDMCS attachment continues even after 19 h. Silane attachment to the substrate surface is driven by hydrolysis.[11] Silanes with an amine group can self-catalyze the hydrolysis reaction.[50] This might explain why APDMES (Figure 3A) forms a monolayer faster than PDMCS, which lacks an amine.

Figure 5B also shows the $\%Si_{PDMCS}$ from the mixed monolayers as a function of PDMCS exposure time that is calculated using

$$\%Si_{PDMCS} = \%Si_{silane} - \%Si_{APDMES} \quad (6)$$

where $\%Si_{silane}$ is calculated using eq 5, and $\%Si_{APDMES}$ is calculated using the measured %N in Figure 5A and eq 2. Figure 5B shows that $\%Si_{PDMCS}$ in the pure PDMCS monolayer and the calculated $\%Si_{PDMCS}$ (from eq 6) in the mixed monolayer are closely equal at all PDMCS deposition times. This confirms that APDMES does not displace PDMCS that is already attached to the surface, and that our thin films are truly mixed monolayers.

Our control over surface functionality with the mixed monolayer extends previous work in which the stepwise deposition method was recommended over codeposition techniques to generate mixed monolayers containing chloro- and alkoxysilanes.

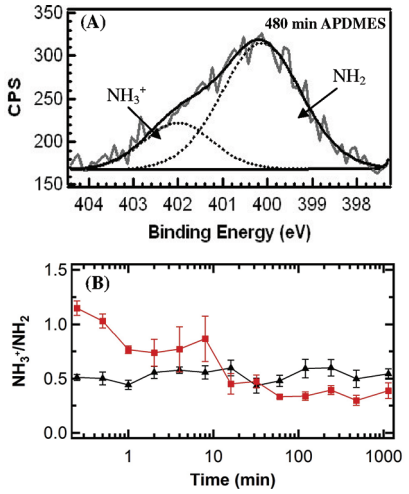

Figure 6. (A) N 1s high-resolution XPS spectrum for a pure APDMES monolayer after a 480 min deposition time. Two nitrogen component peaks are observed in the aminosilane films. (B) Dependence on exposure time of NH_3^+/NH_2 ratio (calculated from N 1s high-resolution XPS spectra) in pure APDMES (red squares) and PDMCS/APDMES mixed monolayers (black triangles). The *x*-axis for the mixed monolayer curve is PDMCS exposure time.

Stepwise deposition provides better control whenever the kinetics of attachment of the two silanes are different.[51]

The high-resolution XPS N 1s spectrum, shown in Figure 6A, shows the two nitrogen component peaks present in our pure APDMES films, a free amine ($-NH_2$, 399.9 ± 0.1 eV) and a protonated amine ($-NH_3^+$, 401.9 ± 0.1 eV). These two species are observed in all spectra for both pure APDMES and PDMCS/APDMES mixed monolayers and were previously observed in other aminosilane films.[52] The free amine is reactive due to its lone pair electrons, whereas the protonated amine is not.[53] The protonated amine component peak is attributed to interactions between the APDMES amine groups and surface silanols on the silica substrate, resulting in proton transfer to the amine group.[53] From these high-resolution XPS N 1s spectra, we calculate the NH_3^+/NH_2 ratio by dividing the percent area of the NH_3^+ peak by the percent area of the NH_2 peak. Figure 6B shows the NH_3^+/NH_2 ratio as a function of exposure time for both types of monolayers. In the PDMCS/APDMES mixed monolayer, the NH_3^+/NH_2 ratio remains relatively constant at ~0.5. However, the NH_3^+/NH_2 ratio in pure APDMES monolayers decreases until about 60 min, when it levels off at about 0.35.

Predeposited methyl-terminated silanes have been found to reduce interactions between the amine in aminosilane films and silica surface silanols compared to pure aminosilane monolayers.[10] Here, we observe that the predeposition of PDMCS maintains the degree of interactions between the amine and surface silanols while the interaction in pure APDMES monolayers depends on silane density. PDMCS predeposited on the surface occupies silanol sites, and controls the number of sites available to interact with the APDMES amines.

Effect of Amine Density on DNA Attachment. We use these well-characterized PDMCS/APDMES mixed monolayer samples for DNA probe immobilization and DNA target hybridization. As described below, both probe immobilization and target hybridization fluorescence correlate semiquantitatively to the amine surface density, but they are not yet fully understood.

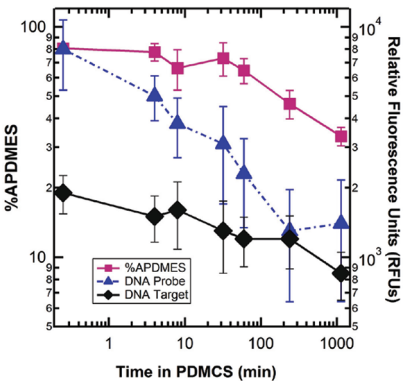

Figure 7. Comparison of %APDMES and the fluorescence from immobilized DNA probes and hybridized DNA targets versus PDMCS deposition time, for PDMCS/APDMES mixed monolayers. %APDMES is from high-resolution XPS, as described in the text.

After the mixed monolayer was attached to the silica surface, the Sulfo-EMCS cross-linker was covalently bonded to an APDMES terminal amine by a nucleophilic substitution at the N-hydroxysuccinimide (NHS) ester. Cross-linker attachment was confirmed by the appearance of an amide carbonyl (C(O)N) component peak in the C 1s high-resolution XPS spectra of the cross-linker-treated samples (see the Supporting Information, Figure S3). In addition, a fluorescence signal was detected when the maleimide terminations of the cross-linker-treated surface were allowed to bind with thiol-modified DNA tagged with a fluorescent molecule. The thiol-free negative controls did not produce any detectable fluorescence signal, indicating negligible nonspecific adsorption of DNA to the surface. Finally, fluorescently tagged cDNA was hybridized to the attached probe DNA. Again, negative controls without a complementary base sequence indicated negligible amounts of nonspecific adsorption.

Figure 7 plots, on a logarithmic scale, the %APDMES versus PDMCS deposition time for the mixed monolayers and shows both the DNA probe and target fluorescence observed on the same samples. %APDMES, the percentage of the mixed monolayer that is composed of APDMES, is calculated using

$$\%\text{APDMES} = \frac{\%\text{Si}_{\text{APDMES}}}{\%\text{Si}_{\text{silane}}} * 100\% \quad (7)$$

where $\%\text{Si}_{\text{APDMES}}$ is calculated using eq 2 and $\%\text{Si}_{\text{silane}}$ is calculated using eq 5. Both the DNA probe and the target fluorescence decrease with decreased %APDMES in the mixed monolayer. A factor of 2 reduction in the percentage of APDMES on the surface results in a roughly a factor of 5 decrease in probe fluorescence and a factor of 2 decrease in the target fluorescence. Thus, the target DNA fluorescence follows the amine density as might be expected, but the probe fluorescence falls faster than the amine density.

Some fluorescence-based DNA assays are known to have molecular quantification limitations[37] because of fluorophore intermolecular interactions that can lead to self-quenching[37,54,55] or fluorescence resonance energy transfer (FRET).[56] However, these effects are unlikely to limit the hybridization fluorescence observed here, because it is a factor of 4 below immobilization fluorescence levels that we are observing successfully.

One of the metrics used for evaluating the performance of DNA microarrays is hybridization efficiency, which we take to be the ratio of the DNA target fluorescence signal to the DNA probe signal. As seen from Figure 7, the hybridization efficiency is

relatively low at short PDMCS treatments times, but then gradually increases and reaches its maximum when the %APDMES in the mixed monolayer is below about 50%.

Many previous studies using other surface functionalization chemistries,[27,28,57−59] found that lower probe densities resulted in higher hybridization efficiencies. Gao et al. suggest that immobilized probes confined on a substrate surface can present steric and electrostatic hindrances to hybridization.[60] At high probe densities, when they are packed more tightly, these hindrances to hybridization are likely made worse, for example by intrinsic disorder within the DNA probe film.[61] These studies highlight the complexity of the surface kinetics of DNA attachment; additionally, other factors such as DNA probe orientation on the surface,[62] formation of secondary structures in the ssDNA probe or target,[60] ionic strength of the hybridization solution[29] and probe−probe interactions[30] can play a role. Despite all these complications, we find (Figure 7) that DNA attachment is strongly influenced by the amine density in the mixed monolayer, as demonstrated by the decrease of both the DNA probe and target fluorescence signals with the density of APDMES amine sites.

CONCLUSIONS

We have demonstrated that the $Si(-O)_1$ high-resolution XPS peak area within the Si 2p peak effectively quantifies the relative silane surface coverage on silica and can be used to quantify silanes without elementally unique functional groups. The technique permits us to determine the fraction of APDMES amine-bearing molecules in PDMCS/APDMES mixed monolayers. Surface amine density is controlled in both pure APDMES and PDMCS/APDMES mixed monolayers. DNA hybridization efficiencies increase with decreasing probe density for the mixed monolayers and the degree of DNA target hybridization roughly follows the surface amine density.

ASSOCIATED CONTENT

Supporting Information. Additional XPS spectra, AFM images, and a pdf file of ref 33. This material is available free of charge via the Internet at http://pubs.acs.org.

AUTHOR INFORMATION

Corresponding Author
*E-mail: Howard.Branz@nrel.gov.

ACKNOWLEDGMENT

We acknowledge the National Renewable Energy Laboratory (NREL) Laboratory Directed Research and Development for funding this project as part of DOE Contract #DE-AC36-99GO10337. We are very appreciative of Neal Fairley, who developed CasaXPS software, for all his advice regarding analysis of XPS spectra. We also thank Patrick McCurdy and Colorado State University for access to their XPS instrument. We thank Bobby To and Helio Moutinho at NREL, who performed the AFM analyses. Finally, we thank Stephen Boyes for helpful suggestions on surface chemistry.

REFERENCES

(1) Daehler, A.; Boskovic, S.; Gee, M. L.; Separovic, F.; Stevens, G. W.; O'Connor, A. J. *J. Phys. Chem. B* **2005**, *109*, 16263–71.
(2) Dejeu, J.; Gauthier, M.; Rougeot, P.; Boireau, W. *ACS Appl. Mater. Interfaces* **2009**, *1*, 1966–73.
(3) Hoff, J. D.; Cheng, L.-J.; Meyhofer, E.; Guo, J.; Hunt, A. J. *Nano Lett.* **2004**, *4*, 853–857.
(4) Hoffmann, C.; Tovar, G. E. *J. Colloid Interface Sci.* **2006**, *295*, 427–35.
(5) Jin, L.; Horgan, A.; Levicky, R. *Langmuir* **2003**, *19*, 6968–6975.
(6) Jones, K. *J. Chromatogr.* **1987**, *392*, 1–10.
(7) Jones, K. *J. Chromatogr.* **1987**, *392*, 11–16.
(8) Oh, S. J.; Cho, S. J.; Kim, C. O.; Park, J. W. *Langmuir* **2002**, *18*, 1764–1769.
(9) Wazawa, T.; Ishizuka-Katsura, Y.; Nishikawa, S.; Iwane, A. H.; Aoyama, S. *Anal. Chem.* **2006**, *78*, 2549–56.
(10) Harder, P.; Bierbaum, K.; Woell, C.; Grunze, M. *Langmuir* **1997** *13*, 445–454.
(11) Silberzan, P.; Leger, L.; Ausserre, D.; Benattar, J. J. *Langmuir* **1991**, *7*, 1647–1651.
(12) Choi, I.; Kim, Y.; Kang, S. K.; Lee, J.; Yi, J. *Langmuir* **2006**, *22*, 4885–9.
(13) Howarter, J. A.; Youngblood, J. P. *Langmuir* **2006**, *22*, 11142–7.
(14) Fadeev, Y. A.; McCarthy, T. J. *Langmuir* **1999**, *15*, 7238–7243.
(15) Wang, Y.; Cai, J.; Rauscher, H.; Behm, R. J.; Goedel, W. A. *Chemistry* **2005**, *11*, 3968–78.
(16) Lee, I.; Wool, R. P. *Thin Solid Films* **2000**, *379*, 94–100.
(17) Briggs, D.; Grant, J. T. *Surface Analysis by Auger and X-Ray Photoelectron Spectroscopy*; IM Publications and SurfaceSpectra Limited: Trowbridge, U.K., 2003.
(18) Pleul, D.; Frenzel, R.; Eschner, M.; Simon, F. *Anal. Bioanal. Chem.* **2003**, *375*, 1276–81.
(19) Moulder, J. F.; Stickle, W. F.; Sobol, P. E.; Bomben, K. D. *Handbook of X-ray Photoelectron Spectroscopy*; Physical Electronics, Inc.: Eden Prairie, MN, 1995.
(20) Alexander, M. R.; Short, R. D.; Jones, F. R.; Michaeli, W.; Blomfield, C. J. *Appl. Surf. Sci.* **1999**, *137*, 179–183.
(21) Zhang, J.; Wavhal, D. S.; Fisher, E. R. *J. Vac. Sci. Technol., A* **2004**, *22*, 201–213.
(22) Bellel, A.; Sahli, S.; Raynaud, P.; Segui, Y.; Ziari, Z.; Eschaich, D.; Dennler, G. *Plasma Process. Polym.* **2005**, *2*, 586–594.
(23) Gruniger, A.; Bieder, A.; Sonnenfeld, A.; von Rohr, P. R.; Muller, U.; Hauert, R. *Surf. Coat. Technol.* **2006**, *200*, 4564–4571.
(24) Shearer, J. C.; Fisher, M. J.; Hoogeland, D.; Fisher, E. R. *Appl. Surf. Sci.* **2010**, *256*, 2081–2091.
(25) O'Hare, L.-A.; Parbhoo, B.; Leadley, S. R. *Surf. Interface Anal.* **2004**, *36*, 1427–1434.
(26) Riepl, M.; Enander, K.; Liedberg, B. *Langmuir* **2002**, *18* 7016–7023.
(27) Peterson, A. W.; Heaton, R. J.; Georgiadis, R. M. *Nucl. Acids Res.* **2001**, *29*, 5163–8.
(28) Cattaruzza, F.; Cricenti, A.; Flamini, A.; Girasole, M.; Longo, G.; Prosperi, T.; Andreano, G.; Cellai, L.; Chirivino, E. *Nucl. Acids Res.* **2006**, *34*, e32.
(29) Gong, P.; Levicky, R. *Proc. Natl. Acad. Sci. U.S.A.* **2008**, *105*, 5301–6.
(30) Mocanu, D.; Kolesnychenko, A.; Aarts, S.; Dejong, A. T.; Pierik, A.; Coene, W.; Vossenaar, E.; Stapert, H. *Anal. Biochem.* **2008**, *380*, 84–90.
(31) Riccelli, P. V.; Merante, F.; Leung, K. T.; Bortolin, S.; Zastawny, R. L.; Janeczko, R.; Benight, A. S. *Nucl. Acids Res.* **2001**, *29*, 996–1004.
(32) Pasternack, R. M.; Amy, S. R.; Chabal, Y. J. *Langmuir* **2008**, *24*, 12963–12971.
(33) Scientific, T. EMCS and Sulfo-EMCS. http://www.piercenet.com/files/1761kc9.pdf (accessed 8/11/2010). PDF file can be found in the Supporting Information at http://pubs.acs.org.
(34) Wasserman, S. R.; Tao, Y.-T.; Whitesides, G. M. *Langmuir* **1989**, *5*, 1074–1087.
(35) Le Grange, J. D.; Markham, J. L. *Langmuir* **1993**, *9*, 1749–1753.
(36) Wagner, C. D.; Riggs, W. M.; Davis, L. E.; Moulder, J. F.; Muilenberg, G. E. *Handbook of X-Ray Photoelectron Spectroscopy*; Perkin-Elmer Corporation: Eden Prairie, MN, 1979.

(37) Gong, P.; Harbers, G. M.; Grainger, D. W. *Anal. Chem.* **2006**, *78*, 2342–51.
(38) Repeated 19 h APDMES exposures show a low standard deviation of $\%Si_{APDMES}$ so we use this as our standard exposure time for the mixed monolayer films discussed in the following section.
(39) Moses, P. R.; Wier, L. M.; Lennox, J. C.; Finklea, H. O.; Lenhard, J. R.; Murray, R. W. *Anal. Chem.* **1978**, *50*, 576–585.
(40) Horr, T. J.; Arora, P. S. *Colloids Surf., A* **1997**, *126*, 113–121.
(41) Alexander, M. R.; Short, R. D.; Jones, F. R.; Stollenwerk, M.; Zabold, J.; Michaeli, W. *J. Mater. Sci.* **1996**, *31*, 1879–1885.
(42) Norstrom, A. E. E.; Fagerholm, H. M.; Rosenholm, J. B. *J. Adhes. Sci. Technol.* **2001**, *15*, 665–679.
(43) Bramblett, A. L.; Boeckl, M. S.; Hauch, K. D.; Ratnre, B. D.; Sasaki, T.; Rogers, J. W., Jr. *Surf. Interface Anal.* **2002**, *33*, 506–515.
(44) Vickerman, J. C., *Surface Analysis—The Principal Techniques*; John Wiley & Sons: Chichester, U.K., 1997.
(45) Peterson, K. E. *IEEE Trans. Electron Devices* **1978**, *ED-25*, 1241–1250.
(46) Petrovykh, D. Y.; Sullivan, J. M.; Whitman, L. J. *Surf. Interface Anal.* **2005**, *37*, 989–997.
(47) Martin, I. T.; Dressen, B.; Boggs, M.; Liu, Y.; Henry, C. S.; Fisher, E. R. *Plasma Process. Polym.* **2007**, *4*, 414–424.
(48) Zhuralev, L. T. *Langmuir* **1987**, *3*, 316–318.
(49) Kallury, K. M. R.; Macdonald, P. M.; Thompson, M. *Langmuir* **1994**, *10*, 492–499.
(50) Vandenberg, E. T.; Bertilsson, L.; Liedberg, B.; Uvdal, K.; Erlandsson, R.; Elwing, H.; Lundström, I. *J. Colloid Interface Sci.* **1991**, *147*, 103–118.
(51) Yang, S.-R.; Kolbesen, B. O. *Appl. Surf. Sci.* **2008**, *25*, 1726–1735.
(52) Moon, J. H.; Kim, J. H.; Kim, K.-j.; Kang, T.-H.; Kim, B.; Kim, C.-H.; Hahn, J. H.; Park, J. W. *Langmuir* **1997**, *13*, 4305–4310.
(53) White, L. D.; Tripp, C. P. *J. Colloid Interface Sci.* **2000**, *232*, 400–407.
(54) Guo, Z.; Guilfoyle, R. A.; Thiel, A. J.; Wang, R.; Smith, L. M. *Nucl. Acids Res.* **1994**, *22*, 5456–65.
(55) Zhuang, X.; Ha, T.; Kim, H. D.; Centner, T.; Labeit, S.; Chu, S. *Proc. Natl. Acad. Sci. U.S.A.* **2000**, *97*, 14241–4.
(56) Lee, L. G.; Connell, C. R.; Bloch, W. *Nucl. Acids Res.* **1993**, *21*, 3761–3766.
(57) Mir, M.; Alvarez, M.; Azzaroni, O.; Knoll, W. *Langmuir* **2008**, *24*, 13001–6.
(58) Chen, S.; Phillips, M. F.; Cerrina, F.; Smith, L. M. *Langmuir* **2009**, *25*, 6570–5.
(59) Malic, L.; Veres, T.; Tabrizian, M. *Biosens. Bioelectron.* **2009**, *24*, 2218–24.
(60) Gao, Y.; Wolf, L. K.; Georgiadis, R. M. *Nucl. Acids Res.* **2006**, *34*, 3370–7.
(61) Mirmomtaz, E.; Castronovo, M.; Grunwald, C.; Bano, F.; Scaini, D.; Ensafi, A. A.; Scoles, G.; Casalis, L. *Nano Lett.* **2008**, *8*, 4134–9.
(62) Lee, C. Y.; Gamble, L. J.; Grainger, D. W.; Castner, D. G. *Biointerphases* **2006**, *1*, 82–92.